

Particle-Motion Attractors due to Particle-Boundary Interaction in Incompressible Steady Three-Dimensional Cavity Flow

H. C. Kuhlmann¹, F. Romanò¹, H. Wu¹ and S. Albensoeder²

¹Institute of Fluid Mechanics and Heat Transfer, TU Wien, 1060 Vienna, Austria

²School of Mathematics and Science, Carl von Ossietzky Universität, 26111 Oldenburg, Germany

Abstract

The incompressible steady three-dimensional flow in a two-sided anti-symmetrically lid-driven cavity and the motion of a finite-size spherical particle is investigated. The flow field is calculated numerically using a fully spectral code allowing to identify regions of chaotic and regular streamlines. The motion of a finite-size particle which is density-matched to the fluid is calculated approximating its motion by advection in the bulk and by inelastic collisions near the boundaries. The limit cycle found for the particle motion is confirmed by experiments using similar parameters. The results demonstrate the general importance of particle–boundary interactions for the creation of particle accumulation structures which can exist in a whole class of incompressible steady three-dimensional flows.

Introduction

It is well known that chaotic and regular streamlines can coexist in steady three-dimensional incompressible Navier-Stokes flows [17, 4]. If the steady three-dimensional flow bifurcates from a steady two-dimensional flow the streamlines usually become chaotic from the boundaries [5], with quasiperiodic motion restricted to Kolmogorov-Arnold-Moser (KAM) tori. When the chaotic layer between the KAM tori and the boundary is locally thin, a suspended particle can be trapped in or near the regular region [10, 15, 14]. In case many particles are trapped the corresponding periodic orbit or the quasiperiodic particle orbits can easily be identified visually in experiments. The emerging dissipative structures, first observed in thermocapillary liquid bridges [19], are called particle-accumulation structures (PAS) [23, 20]. While a particle trapping can be caused entirely by inertia due to the density difference between particle and fluid [24, 16], the accumulation can be more rapid if it is assisted or even exclusively caused by the repulsive forces a particle experiences close to a boundary [18, 16].

Here we consider the steady flow in a two-sided anti-symmetrically lid-driven cavity [3]. A three-dimensional cel-

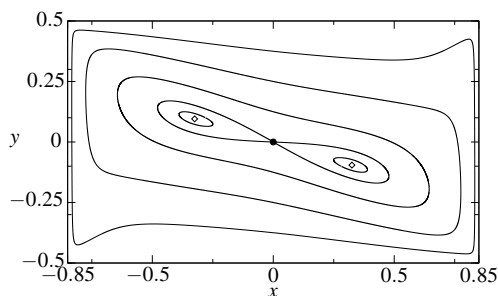


Figure 1: Streamlines of the two-dimensional flow at criticality $Re = Re_c = 211.53$ for aspect ratio $\Gamma = 1.7$. The boundary at the left and the right move upward and downward, respectively. Dot and diamonds indicate hyperbolic and elliptic stagnation points, respectively.

lular flow arises due to the elliptic instability of the basic two-dimensional strained vortex [12, 1]. We discuss the topological features of the flow including the KAM tori and numerically simulate the motion of neutrally-buoyant particles subject to particle–boundary interaction. The numerically predicted particle–motion attractors are compared with experimental data.

Definition of the problem

We consider a Newtonian fluid with density ρ_f and kinematic viscosity ν in a cavity of rectangular cross-section infinitely extended in direction normal to it. The fluid motion is driven by two facing walls which move tangentially in opposite directions with the same constant velocity magnitude U (figure 1). The steady motion is governed by the incompressible Navier–Stokes and continuity equations

$$\vec{u} \cdot \nabla \vec{u} = -\nabla p + \nabla^2 \vec{u}, \quad (1a)$$

$$\vec{u} = 0. \quad (1b)$$

where we use the length, velocity and pressure scales h , ν/h and $\rho_f \nu^2/h^2$, respectively, where h is the height of the cavity. In the (x, y) plane the boundary conditions are $\vec{u}(x, y = \pm 1/2, z) = 0$, $\vec{u}(x = \pm \Gamma/2, y, z) = \mp Re$, where $\Gamma = d/h = 1.7$ is the aspect ratio (width-to-height ratio) and the Reynolds number is defined as

$$Re = \frac{Uh}{\nu}. \quad (2)$$

Figure 1 shows streamlines of the basic flow at criticality. As the Reynolds number is increased beyond $Re_c(\Gamma = 1.7) = 211.53$ the flow becomes three-dimensional [1] with respect to a steady cellular flow. In the third (z) direction we thus impose periodic boundary conditions $\vec{u}(x, y, \lambda/2) = \vec{u}(x, y, -\lambda/2)$, where $\lambda = \lambda_c = 2.73$ is selected as the critical wavelength for the onset of the three-dimensional steady flow. The supercritical steady rectangular convection cells are very robust for a large range of Reynolds numbers [6].

Solution techniques

Equations (1a) are solved with a full spectral $\mathcal{P}_N - \mathcal{P}_{N-2}$ method [7] using Chebyshev polynomials in x and y and harmonics in z . To reduce the corner singularities the analytical approximation up to second order [8, 9] of the asymptotic solution to the corner flow have been taken into account. The code has been extensively tested and verified [2]. For all calculations a resolution of 128^3 collocation points was used.

To calculate the streamlines $\vec{X}(t)$ the advection equation $\dot{\vec{X}} = \vec{u}(x, y, z)$ is solved using a 4th-/5th-order Runge–Kutta Dormand–Prince method with adaptive time stepping. The absolute and relative errors per time step are always less than 10^{-10} . To solve the advection equation the flow needs to be interpolated. Depending on the accuracy required either a linear interpolation is employed between the functional values on the

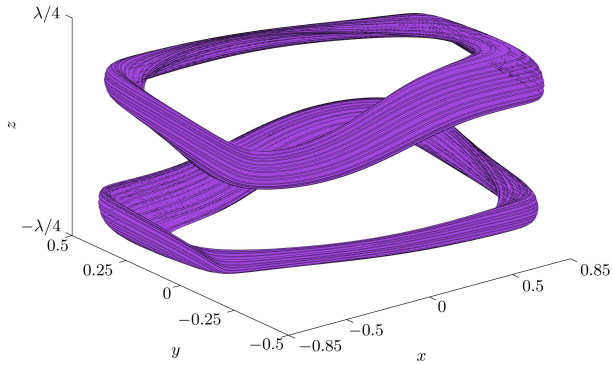


Figure 2: A pair of KAM tori for $Re = 400$.

spectral grid, or the full spectral approximation is used which is computationally more expensive.

In order to model the motion of density-matched finite-size spherical particles moving in the cavity, the particle–surface interaction (PSI) model is used [10, 14]. In this model particles move like fluid elements except near the boundaries where they are assumed to experience an inelastic collision in direction normal to the walls when their centroids approach any boundary up to a minimum distance given by the particle radius a increased by a lubrication gap δ . This yields a layer on each wall, inaccessible by the particle centroids, of thickness $\Delta = a + \delta$, called interaction length. After the collision and as long as the wall-normal velocity is directed toward the wall the particle is assumed to slide along the wall until the wall-normal velocity turns inward. At this point the particle is released to the bulk.

Results

Fluid motion

The nonlinear steady fluid motion in a single rectangular convective cell comprising half a wavelength of the flow pattern is found to be point symmetric with respect to the center of the cell, as in experiments [6]. The flow consists of chaotic and regular streamlines. As the Reynolds number is increased beyond the critical value chaotic streamlines invade the cell from the boundaries. The regular motion is confined to KAM tori which were identified using Poincaré sections. From these we could identify the largest reconstructible KAM tori. For low supercritical Reynolds numbers we find a single pair of point-symmetric KAM tori. An example is shown in figure 2 for $Re = 400$. As the Reynolds number is increased each torus splits into two. For $Re = 700$, e.g., two of the resulting tori are similar, but more slender, as the ones shown in figure 2. The two other tori are each winding about the respective main tori with winding number one (not shown).

The minimum distance Δ_L of the closed streamlines inside of the KAM tori from the boundary is an important parameter for accumulation of particles in the framework of the PSI model [15]. In all cases the minimum distance of the closed streamlines arises with respect to the moving wall. For $Re = 400$ we find $\Delta_L = 0.0711$.

Particle motion

Inertia effects on the particle motion are very weak for small particles density-matched to the fluid. In that case the time required for inertial clustering scales like $\sim \rho / (|\rho - 1|St)$ [16], where $\rho = \rho_p / \rho_f$ is the particle-to-fluid density ratio and $St = 2\rho a^2 / 9$ the viscously-scaled Stokes number with a the dimensionless particle radius.

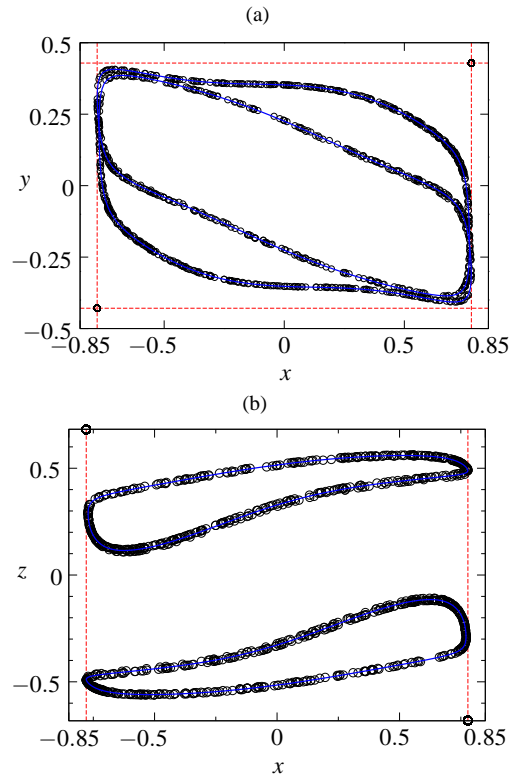


Figure 3: Accumulation of particles (represented by small dots) at $t = 1$ on a limit cycle (colored line) for $Re = 400$ and $\Delta = \Delta_L = 0.0711$ projected on the (x, y) - (a) and (x, z) -plane (b). The red dashed lines indicate $x = x^*$. 2500 particles have been used with random initial conditions.

Here we are interested in the effect of the finite-particle size alone and consider $\rho = 1$. If the variation of the velocity over the length scale of the particle is small compared to the flow velocity at its centroid a density-matched particle essentially follows the flow. We assume this condition to hold, except near the boundaries. Therefore the particle motion is approximated by advection in the bulk. Near the boundaries the PSI model is applied. This type of modeling is motivated in order to capture the key effect of the boundary on the particle motion.

According to [10] and [15] a perfect periodic attractor for the particle motion exists in the case when the closed streamline of a KAM torus is tangent to the collision plane characterized by $|x^*| = \Gamma/2 - \Delta$. In that case the particles cluster on the closed streamline. For an interaction length $\Delta = \Delta_L$ the projection of the positions of initially randomly distributed particle is shown in figure 3 after having evolved for $t = 1$. As in similar investigations [11, 16], the particles are assumed to move independently of each other. The number of particles only serves the purpose of visualization and statistical representation of the attraction dynamics from random initial conditions which, for dilute suspensions, is a one-particle phenomenon.

A simplified explanation of the phenomenon is as follows. Due to the ergodicity of particles initially moving in the chaotic sea they will eventually interact with one of the moving walls. Upon an inelastic collision on $x = x^*$ with one of the moving walls the particle can be released to the bulk inside of the regular region. Once in a regular region, the particle cannot escape from it any more and will be further focussed to a limit cycle by repeated wall interactions, as described by [10]. Depending on the particle size and the structure and location of the KAM tori this process can be more complicated [14].

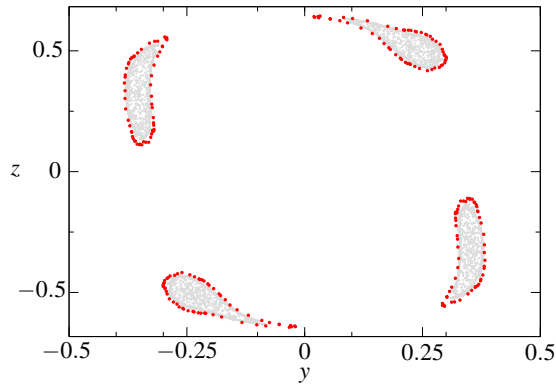


Figure 4: Poincaré section during $t \in [0.75, 1]$ at $x = 0$ of 2500 trajectories (grey dots) for $Re = 400$ and $\Delta = 0.04$. The largest KAM torus is shown by red dots (regular streamlines). Random initial conditions at $t = 0$.

Within this picture the problem contains two time scales. One time scale is related to the transfer of the particle from the chaotic sea to the regular region. The other time scale is related to the focussing inside the regular region. Both times scales should be proportional to a characteristic eddy turnover time τ which can be estimated as h/U . The limiting process, however, is expected to be the transfer of the particle from the chaotic to the regular region of the flow. This process depends crucially on the linear dimension perpendicular to the flow of the intersection set between the KAM tube and the collision planes $x = |x^*|$ (red dashed lines in figure 3) as well as on the degree of mixing in the chaotic region.

If $\Delta_L > \Delta$ the non-inertial particles from outside of the KAM torus which is tangent to x^* in one point are attracted to this particular KAM torus, while particles with centroids inside this KAM torus do not interact with the boundary in the framework of the PSI model. This attraction to a torus is shown in figure 4 for $Re = 400$ and $\Delta = 0.04$. Such accumulation structure has been termed *tubular PAS* [10, 15]. If, on the other hand, $\Delta_L < \Delta$ we find a period doubling of the attractor (not shown), similar as in Ref. [14] for particles in thermocapillary liquid bridges.

Experimental evidence

While the results based on particle advection and the PSI model are quite idealized, in particular, regarding the particle–boundary interaction, see e.g. [18], we found experimental evidence for particle accumulation. For the experiments we employed the same lid-driven cavity as in Siegmann-Hegerfeld et al. [21, 22]. In this experiment the moving walls have been realized by rotating, parallel cylinders of relatively large radii. The experimental aspect ratio based on the mean of the minimum and maximum gap widths (due to the wall curvature) was $\Gamma = 1.6$. The cavity height was 40.1 mm and the fluid was Baysilone silicone oil M20.

Figure 5 shows the trajectory of a particle made from polyethylene with relative density $\rho = 0.99$ and non-dimensional radius $a = 0.05$ (the real particle radius was 1.995 mm) in the flow at $Re = 400$. Taking into account a certain, yet undetermined, lubrication gap between particle and walls the interaction parameter must satisfy $\Delta > a = 0.05$. The experiment was started from rest with a single particle. After 30 minutes the trajectory of the particle was determined using particle tracking. The particle position was recorded for about 100 s at a sampling frequency of 20 Hz. This corresponds to about 35 particle revolutions in the recirculating flow.

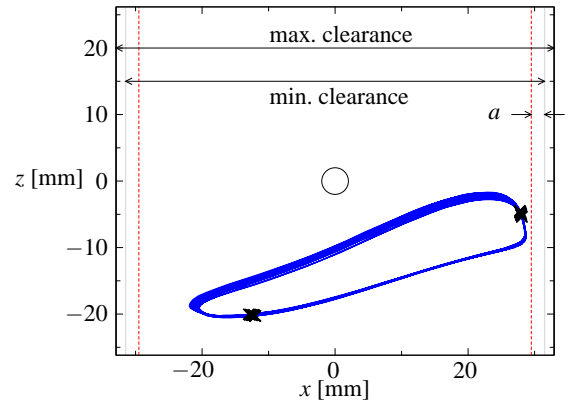


Figure 5: Projection of the orbit (blue) of the centroid of a particle (size indicated by the circle) in the (x, z) plane for $Re = 400$. The markers (\times) are Poincaré points on $y = 0$ of the orbit. Top and bottom mark the boundaries of the convection cell. The minimum cavity width (at $y = 0$) due to wall curvature is indicated by the vertical grey lines. The red dashed lines indicates the minimum distance a particle of radius a can have from the moving wall at the midplane $y = 0$.

Within the remaining small error for the particle trajectory the particle has settled to a limit cycle. As expected from the modeling the limit cycle is in close neighborhood of one of the moving walls. The lubrication gap between the particle and the moving wall can be estimated from the particle size which is indicated by a circle. Note that another limit cycle exists in the experiment as well, which is obtained by reflecting the shown limit cycle at the center of the cell.

The location and shape of the experimental limit cycle is in qualitative agreement with the numerical modeling. Remaining differences can be due to the slightly different aspect ratio, the slightly curved walls in the experiment, the unknown lubrication gap, and the approximations made in the numerical modeling. The relatively good agreement between experimental and numerical result suggests, however, that the fundamental mechanism of particle accumulation by particle–surface interaction is well captured.

Conclusions

Numerical simulations and experiments have been carried out for the motion of a finite-size non-inertial spherical particle in a two-sided anti-symmetrically lid-driven cavity. It was shown that a limit cycle for the particle motion exists. A characteristic feature of the limit cycle is its vicinity to the closed streamline of a KAM torus of the three-dimensional steady flow which takes the particle very close to the moving boundary. As shown by the numerical analysis the limit cycle is essentially created by particle–surface interactions. Inertial effects due to the density difference between particle and fluid can largely be ruled out as a reason for the creation of the limit cycle in the experiment, since the density difference of 1% is very small.

The attraction to the limit cycle is a single-particle process, and not a collective phenomenon. In principle, many individual particles can be attracted to the same limit cycle. However, owing to the relatively large size of the particle used in the present investigation, particle–particle interactions may not always be negligible. The particle–particle interaction may lead to a weakly chaotic particle motion in or near the KAM torus up to a complete suppression of particle accumulation for large particle volume fractions.

The results demonstrate that particle accumulation (PAS) is not restricted to thermocapillary liquid bridges for which it has been studied quite extensively [23, 20, 10, 13, 14]. Therefore, PAS is a general phenomenon which can arise in three-dimensional incompressible flows steady in some frame of reference. Furthermore, our investigation for a nearly density-matched particle confirms the existence of a limit cycle by means of a non-inertial mechanism. To clarify the relative importance of inertia as compared to particle-surface interaction further simulations, similar to Ref. [16], and experiment for heavy particles are in order. It would also be of interest to probe PAS in other laminar three-dimensional flows.

References

- [1] Albensoeder, S. and Kuhlmann, H. C., Linear stability of rectangular cavity flows driven by anti-parallel motion of two facing walls, *J. Fluid Mech.*, **458**, 2002, 153–180.
- [2] Albensoeder, S. and Kuhlmann, H. C., Accurate three-dimensional lid-driven cavity flow, *J. Comput. Phys.*, **206**, 2005, 536–558.
- [3] Albensoeder, S., Kuhlmann, H. C. and Rath, H. J., Multiplicity of steady two-dimensional flows in two-sided lid-driven cavities, *Theor. Comp. Fluid Dyn.*, **14**, 2001, 223–241.
- [4] Aref, H., Chaotic advection of fluid particles, *Philosophical Transactions of the Royal Society of London. Series A: Physical and Engineering Sciences*, **333**, 1990, 273–288.
- [5] Biemond, J. J. B., de Moura, A. P. S., Károlyi, G., Grebogi, C. and Nijmeijer, H., Onset of chaotic advection in open flows, *Phys. Rev. E*, **78**, 2008, 016317–1–016317–5.
- [6] Blohm, C. and Kuhlmann, H. C., The two-sided lid-driven cavity: Experiments on stationary and time-dependent flows, *J. Fluid Mech.*, **450**, 2002, 67–95.
- [7] Botella, O. and Peyret, R., Benchmark spectral results on the lid-driven cavity flow, *Comp. Fluids*, **27**, 1998, 421–433.
- [8] Gupta, M. M., Manohar, R. P. and Noble, B., Nature of viscous flows near sharp corners, *Comp. Fluids*, **9**, 1981, 379–388.
- [9] Hancock, C., Lewis, E. and Moffatt, H. K., Effects of inertia in forced corner flows, *J. Fluid Mech.*, **112**, 1981, 315–327.
- [10] Hofmann, E. and Kuhlmann, H. C., Particle accumulation on periodic orbits by repeated free surface collisions, *Phys. Fluids*, **23**, 2011, 0721106–1–0721106–14.
- [11] Kuhlmann, H. C. and Muldoon, F. H., Particle-accumulation structures in periodic free-surface flows: Inertia versus surface collisions, *Phys. Rev. E*, **85**, 2012, 046310–1–046310–5.
- [12] Kuhlmann, H. C., Wanschura, M. and Rath, H. J., Flow in two-sided lid-driven cavities: Non-uniqueness, instabilities, and cellular structures, *J. Fluid Mech.*, **336**, 1997, 267–299.
- [13] Melnikov, D. E., Pushkin, D. O. and Shevtsova, V. M., Synchronization of finite-size particles by a traveling wave in a cylindrical flow, *Phys. Fluids*, **25**, 2013, 092108–1–092108–21.
- [14] Mukin, R. V. and Kuhlmann, H. C., Topology of hydrothermal waves in liquid bridges and dissipative structures of transported particles, *Phys. Rev. E*, **88**, 2013, 053016–1–053016–20.
- [15] Muldoon, F. H. and Kuhlmann, H. C., Coherent particulate structures by boundary interaction of small particles in confined periodic flows, *Physica D*, **253**, 2013, 40–65.
- [16] Muldoon, F. H. and Kuhlmann, H. C., Origin of particle accumulation structures in liquid bridges: particle–boundary interactions versus inertia, *Phys. Fluids*, **28**, 2016, 073305–1–073305–17.
- [17] Ottino, J. M., *The Kinematics of Mixing: Stretching, Chaos, and Transport*, Cambridge Texts in Applied Mathematics, Cambridge University Press, Cambridge, 1989.
- [18] Romanò, F. and Kuhlmann, H. C., Numerical investigation of the interaction of a finite-size particle with a tangentially moving boundary, *Int. J. Heat Fluid Flow*, **in press**, doi: [10.1016/j.ijheatfluidflow.2016.07.011](https://doi.org/10.1016/j.ijheatfluidflow.2016.07.011).
- [19] Schwabe, D., Hintz, P. and Frank, S., New features of thermocapillary convection in floating zones revealed by tracer particle accumulation structures (PAS), *Microgravity Sci. Technol.*, **9**, 1996, 163–168.
- [20] Schwabe, D., Mizev, A. I., Udhayasankar, M. and Tanaka, S., Formation of dynamic particle accumulation structures in oscillatory thermocapillary flow in liquid bridges, *Phys. Fluids*, **19**, 2007, 072102–1–072102–18.
- [21] Siegmann-Hegerfeld, T., Albensoeder, S. and Kuhlmann, H. C., Two- and three-dimensional flows in nearly rectangular cavities driven by collinear motion of two facing walls, *Exp. Fluids*, **45**, 2008, 781–796.
- [22] Siegmann-Hegerfeld, T., Albensoeder, S. and Kuhlmann, H. C., Three-dimensional flow in a lid-driven cavity with width-to-height ratio of 1.6, *Exp. Fluids*, **54**, 2013, 1526–1–1526–10.
- [23] Tanaka, S., Kawamura, H., Ueno, I. and Schwabe, D., Flow structure and dynamic particle accumulation in thermocapillary convection in a liquid bridge, *Phys. Fluids*, **18**, 2006, 067103–1–067103–11.
- [24] Yarin, A. L., Kowalewski, T. A., Hiller, W. J. and Koch, S., Distribution of particles suspended in convective flow in differentially heated cavity, *Phys. Fluids*, **8**, 1996, 1130–1140.